

REPORT

A Pleistocene ice core record of atmospheric O₂ concentrations

1. D. A. Stolper^{1,*}
2. M. L. Bender^{1,2}
3. G. B. Dreyfus^{1,3,†}
4. Y. Yan¹
5. J. A. Higgins¹

See all authors and affiliations

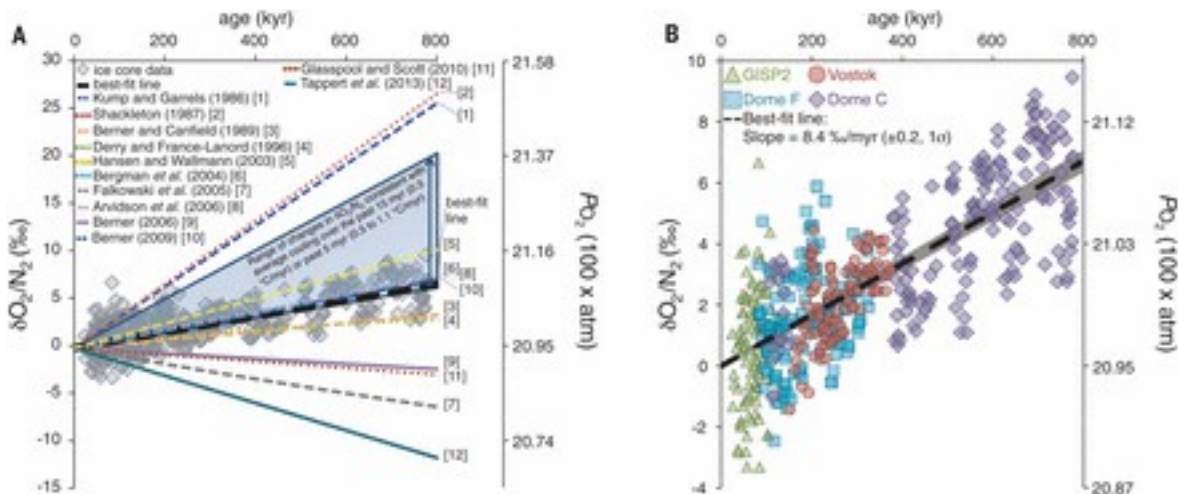
DOI: 10.1126/science.aaf5445

- [**Article**](#)
- [**Figures & Data**](#)
- [**Info & Metrics**](#)
- [**eLetters**](#)
- [**PDF**](#)

Abstract

The history of atmospheric O₂ partial pressures (P_{O_2}) is inextricably linked to the coevolution of life and Earth's biogeochemical cycles. Reconstructions of past P_{O_2} rely on models and proxies but often markedly disagree. We present a record of P_{O_2} reconstructed using O₂/N₂ ratios from ancient air trapped in ice. This record indicates that P_{O_2} declined by 7 per mil (0.7%) over the past 800,000 years, requiring that O₂ sinks were ~2% larger than sources. This decline is consistent with changes in burial and weathering fluxes of organic carbon and pyrite driven by either Neogene cooling or increasing Pleistocene erosion rates. The 800,000-year record of steady average carbon dioxide partial pressures (PCO_2) but declining P_{O_2} provides distinctive evidence that a silicate weathering feedback stabilizes PCO_2 on million-year time scales.

The importance of O₂ to biological and geochemical processes has led to a long-standing interest in reconstructing past atmospheric O₂ partial pressures (P_{O_2} , reported at standard temperature and pressure) ([1–12](#)). However, there is no consensus on the history of Phanerozoic P_{O_2} , with reconstructions disagreeing by as much as 0.2 atm, the present-day pressure of O₂ in the atmosphere (e.g., [7, 10](#)). Even over the past million years, it is not known whether atmospheric O₂ concentrations varied or whether the O₂ cycle was in steady state ([Fig. 1A](#)). Knowledge of P_{O_2} over the past million years could provide new insights into the O₂ cycle on geologic time scales and serve as a test for models and proxies of past P_{O_2} . Here we present a primary record of P_{O_2} over the past 800,000 years, reconstructed using measured O₂/N₂ ratios of ancient air trapped in polar ice.



- [Download high-res image](#)
- [Open in new tab](#)
- [Download Powerpoint](#)

Fig. 1 $\delta\text{O}_2/\text{N}_2$ and P_{O_2} values versus age from ice cores and from model and proxy predictions.

(A) Comparison of the ice core data with model and proxy predictions (1–12). (B) $\delta\text{O}_2/\text{N}_2$ versus ice age from ice cores. $\delta\text{O}_2/\text{N}_2$ decreases by 8.4‰ per million years ($\pm 0.2, 1\sigma$). Gray bands are 95% confidence intervals. Data are corrected for gravitational, interlaboratory, and bubble close-off fractionations (19). kyr, thousand years; myr, million years.

O_2/N_2 ratios of this kind have been extensively used to date ice cores on the basis of the correlation between O_2/N_2 and local summertime insolation (13–17). Despite being directly tied to atmospheric compositions, O_2/N_2 ratios have never before been used to reconstruct past P_{O_2} . Landais *et al.* (16) and Bazin *et al.* (17), while using O_2/N_2 ratios for ice core dating, noted a decline in O_2/N_2 values with time (i.e., toward the present). They suggested that this decline could be due to secular changes in air entrapment processes, gas loss during core storage, or changes in atmospheric O_2/N_2 , but they did not evaluate these hypotheses. Given the potential for O_2/N_2 ratios to directly constrain Pleistocene P_{O_2} , we present compiled O_2/N_2 measurements from multiple ice core records and evaluate their geochemical implications.

We compiled published O_2/N_2 ice core records from Greenland [Greenland Ice Sheet Project 2 (GISP2) (18)] and Antarctica [Vostok (13), Dome F (14), and Dome C (17); table S1], along with previously unpublished Antarctic Ar/ N_2 records [Vostok and Dome C; table S2]. The data were treated as follows [see (19) for more details]. (i) Measured ratios were corrected for gravitational fractionations and are reported using δ notation

$$\delta O_2/N_2 = 1000 \times \left(\frac{[O_2]/[N_2]_{\text{sample}}}{[O_2]/[N_2]_{\text{preatthropogenic atmosphere}}} - 1 \right) \quad (1)$$

$$\delta Ar/N_2 = 1000 \times \left(\frac{[Ar]/[N_2]_{\text{sample}}}{[Ar]/[N_2]_{\text{modern atmosphere}}} - 1 \right) \quad (2)$$

where brackets denote concentrations. A decrease in $\delta O_2/N_2$ of 1 per mil (\textperthousand) equates to a 0.1% decrease in P_{O_2} relative to the preanthropogenic atmosphere (i.e., the modern atmosphere corrected for fossil fuel combustion). We define the preanthropogenic atmosphere as having $\delta O_2/N_2 = 0\text{\textperthousand}$ and $\delta Ar/N_2 = 0\text{\textperthousand}$. (ii) Only analyses of bubble-free ice with clathrates were considered. (iii) The portions of the $\delta O_2/N_2$ and $\delta Ar/N_2$ signals linked to insolation (13–17) were removed (figs. S1 and S2). (iv) We corrected for differences in bubble close-off fractionations between ice cores and interlaboratory offsets by assuming that, in the absence of such effects, trapped gases of a given age share identical atmospheric O_2/N_2 and Ar/N_2 values (figs. S3 and S4).

The fully corrected data are plotted versus ice age in [Figs. 1B](#) ($\delta O_2/N_2$) and [2A](#) ($\delta Ar/N_2$). $\delta O_2/N_2$ values decrease by 8.4‰ per million years (± 0.2 , 1σ), consistent with the observations of Landais *et al.* (16) and Bazin *et al.* (17). $\delta Ar/N_2$ values increase by 1.6‰ per million years (± 0.2 , 1σ), which is discussed below.

- [Download high-res image](#)
- [Open in new tab](#)
- [Download Powerpoint](#)

Fig. 2 Evidence that the observed decline in $\delta O_2/N_2$ with time does not originate from either secular changes in bubble close-off fractionations or ice core storage.

(A) $\delta Ar/N_2$ and $\delta O_2/N_2$ versus ice age. Bubble close-off processes and gas loss would cause $\delta Ar/N_2$ and $\delta O_2/N_2$ to covary with slopes of 0.3 to 0.6. The observed $\delta Ar/N_2$ trend does not overlap with these expected trends (orange wedge), indicating that such processes did not cause the decline in $\delta O_2/N_2$. (B) Dome C $\delta O_2/N_2$ versus ice age and (C) versus depth. Dotted lines were fit to ice >400,000 years old or >2600 m deep and extrapolated to younger ages or shallower depths. Extrapolations of the fits pass through the younger data (B) but miss the deeper data [beyond 4σ (C)], indicating depth-dependent glacial properties did not cause the decline in $\delta O_2/N_2$. Gray bands are 95% confidence intervals. Data are corrected for gravitational, interlaboratory, and bubble close-off fractionations (19).

The decline in $\delta\text{O}_2/\text{N}_2$ with time could result from temporal changes in bubble entrapment processes, effects of ice core storage, a decline in $P\text{O}_2$, or an increase in the partial pressure of atmospheric N_2 ($P\text{N}_2$). We now evaluate these possibilities in the context of the $\delta\text{O}_2/\text{N}_2$ record.

$\delta\text{O}_2/\text{N}_2$ values of gas extracted from ice are ~ 5 to $10\text{\textperthousand}$ lower than those of ambient air ([13–18](#), [20](#), [21](#)). Additionally, $\delta\text{Ar}/\text{N}_2$ covaries with $\delta\text{O}_2/\text{N}_2$ along slopes of 0.3 to 0.6 (fig. S5) ([19](#), [21](#), [22](#)). These depletions and covariations have been attributed to fractionations created during bubble close-off on the basis of measurements and models of firn air ([20](#), [22](#)) and the covariation of $\delta\text{O}_2/\text{N}_2$ and $\delta\text{Ar}/\text{N}_2$ with local insolatation (figs. S1 and S2) ([13–17](#), [19](#)). If secular changes in bubble close-off fractionations caused the decline in $\delta\text{O}_2/\text{N}_2$, then $\delta\text{Ar}/\text{N}_2$ values should covary with $\delta\text{O}_2/\text{N}_2$ along slopes of 0.3 to 0.6 and thus decline by 2.5 to $5.0\text{\textperthousand}$ per million years. Instead, $\delta\text{Ar}/\text{N}_2$ increases with time by $1.6\text{\textperthousand}$ per million years (± 0.2 , 1σ ; [Fig. 2A](#)). The increasing trend is largely due to a subset of Vostok data from 330,000- to 370,000-year-old ice that is lower in $\delta\text{Ar}/\text{N}_2$ by $\sim 1\text{\textperthousand}$ compared with younger data. Exclusion of this subset yields an increase in $\delta\text{Ar}/\text{N}_2$ with time of only $0.35\text{\textperthousand}$ (± 0.20 , 1σ), within the 2σ error range of no change. Regardless, whichever way the $\delta\text{Ar}/\text{N}_2$ are analyzed, they are inconsistent with the decline in $\delta\text{O}_2/\text{N}_2$ being caused by bubble close-off processes ([Fig. 2A](#)).

Ice core storage, under some conditions, causes the $\delta\text{O}_2/\text{N}_2$ values of trapped gases to decline ([14–17](#)). Thus, the second possibility that we consider is that ice core storage lowered the $\delta\text{O}_2/\text{N}_2$ values so that the slope observed in [Fig. 1](#) is an artifact. For example, a change in $\delta\text{O}_2/\text{N}_2$ correlated with ice age but unrelated to atmospheric compositions could result if the retention of O_2 versus N_2 during storage is a function of pre-coring properties controlled by original ice depths (e.g., in situ temperature, pressure, or clathrate size). We evaluate this possibility by using three approaches. (i) Gas loss during core storage causes $\delta\text{Ar}/\text{N}_2$ to decline at half the rate of $\delta\text{O}_2/\text{N}_2$ ([21](#), [23](#), [24](#)). However, as discussed above, the $\delta\text{Ar}/\text{N}_2$ values are not consistent with such a change ([Fig. 2A](#)). (ii) Because some ice properties (e.g., temperature and pressure) can vary linearly with ice depth, we tested whether the Dome C $\delta\text{O}_2/\text{N}_2$ data are better fit by a linear relationship when plotted against ice age or depth. (We note that only the Dome C ice core's age-depth relationship is sufficiently curvilinear for this test to be useful. We linearly regressed both age and depth against $\delta\text{O}_2/\text{N}_2$ for ice older than $\sim 400,000$ years (i.e., deeper than 2600 m) and extrapolated the fits to younger ages and shallower depths. The extrapolation for age ([Fig. 2B](#)) passes through the younger data, whereas the extrapolation for depth ([Fig. 2C](#)) misses the shallower data (by $>4\sigma$). (iii) Repeat $\delta\text{O}_2/\text{N}_2$ measurements of Vostok ice from the same age interval (150,000 to 450,000 years ago) made 10 years apart ([13](#), [15](#)) differ on average by 6\textperthousand , with longer storage leading to lower $\delta\text{O}_2/\text{N}_2$.

Despite this, regressing $\delta O_2/N_2$ against time yields statistically identical (within 1σ) slopes of $\delta O_2/N_2$ versus age for both data sets (fig. S6).

Collectively, the data and tests presented above provide no support for the observed decrease in $\delta O_2/N_2$ over time being an artifact of either bubble close-off processes as they are currently understood or ice core storage. Consequently, we hypothesize and proceed with the interpretation that the observed decline in $\delta O_2/N_2$ reflects changes in $P O_2$ or $P N_2$. Because N_2 has a billion-year atmospheric lifetime (25), we link the decline in $\delta O_2/N_2$ with time exclusively to a decline in $P O_2$. Our hypothesis is further supported by the observation that data from all four ice cores individually exhibit the same general trends and magnitudes of decreasing $\delta O_2/N_2$ with time (table S3), even though each was drilled, stored, and analyzed differently.

The question raised by this record is why $P O_2$ has decreased by $\sim 7\%$ over the past 800,000 years. Changes in $P O_2$ require imbalances between O_2 sources [dominantly modern sedimentary organic carbon (C_{org}) and pyrite burial] and sinks (dominantly ancient sedimentary C_{org} and pyrite oxidation) (26). Thus, a higher rate of oxidative weathering relative to C_{org} and/or pyrite burial over the past million years could have caused the observed $P O_2$ decline. The ~ 2 -million-year (+1.5/-0.5 million years) (26) geological residence time of O_2 , combined with the decline in $\delta O_2/N_2$ of 8.4% per million years, indicates that O_2 sinks were 1.7% larger than sources over the past 800,000 years (27). We now explore possible causes for this drawdown, examining first the impact of changing erosion rates and second the impact of global cooling on $P O_2$.

Global erosion rates influence the amount of rock weathered (consuming O_2) and sediment buried (releasing O_2). These rates have been suggested to have increased up to 100% in the Pleistocene relative to the Pliocene (28) [though this is debated (29)]. Thus, the possibility exists that increased Pleistocene sedimentary erosion and burial rates affected $P O_2$ levels. Indeed, Torres *et al.* (30) modeled that increasing erosion rates over the past 15 million years enhanced oxidation of sedimentary pyrite relative to burial so that $P O_2$ declined on average by 9 to 25% per million years. This is similar to the decline given by the ice core record (8.4% per million years). We note that whether increasing erosion rates cause $P O_2$ to decline (instead of increase) is unknown (31).

Large increases (e.g., 100%) in Pleistocene erosion rates, if they did occur, likely would have required processes that keep O_2 sources and sinks balanced within $\sim 2\%$ (the observed imbalance). Such processes could include the proposed $P O_2$ -dependent control of C_{org} burial fluxes on sedimentary phosphorus burial rates (32). Alternatively, sedimentary mineral surface area is known to positively correlate with total sedimentary C_{org} and pyrite content (33). Hedges and Kiel (33) proposed that the total eroded and total buried mineral surface areas today are about equal. If this was true in

the past, the conservation of eroded versus newly generated mineral surface area may have acted to balance C_{org} and pyrite weathering and burial fluxes (and thus O_2 fluxes), regardless of global erosion rates ([33](#)).

Alternatively, on the basis of $^{13}C/^{12}C$ and $^{18}O/^{16}O$ records from sedimentary carbonates, Shackleton ([2](#)) proposed that Po_2 declined over the Neogene as a result of oceanic cooling. He suggested the following feedback loop: Cooling increases O_2 solubility. This raises dissolved O_2 concentrations, which increases the volume of ocean sediment exposed to dissolved O_2 and thus also increases global aerobic C_{org} remineralization rates ([33](#)). On million-year time scales, C_{org} burial rates and, therefore, Po_2 and O_2 concentrations decline until seawater O_2 concentrations return to their initial (precooling) levels. At this new steady state, C_{org} burial rates have returned to their original values, but Po_2 is stabilized at a lower value.

Shackleton's hypothesis can be evaluated to first order in the context of the $\delta O_2/N_2$ data by using records of past ocean temperature. Specifically, temperatures in the deep (>1000 m depth) ocean were roughly constant from 24 to 14 million years ago ([34, 35](#)). Assuming an O_2 residence time of ~2 million years and the hypothesis that changes in ocean temperature modulate Po_2 , then O_2 sources and sinks would have been in balance by 14 million years ago. The oceans have cooled on average by $0.3^\circ C$ per million years over the past 14 million years and 0.5° to $1.1^\circ C$ per million years over the past 5 million years ([34, 35](#)). Cooling of 0.3° to $1.1^\circ C$ per million years increases O_2 solubility by ~7 to 25‰ per million years ([36](#)). If dissolved O_2 concentrations remained constant (as this hypothesis requires), such changes in O_2 solubility necessitate a decline in Po_2 of ~7 to 25‰ per million years. These rates bracket the rate of decline given by the ice core record (8.4‰ per million years; [Fig. 1A](#)). We note that deep ocean cooling rates track average marine cooling rates, but not precisely, because modern deep waters form in and thus reflect the temperatures of high latitudes. Regardless, the critical point is that this simple calculation is consistent with the ice core-derived $\delta O_2/N_2$ record and supports the hypothesis that global temperature stabilizes Po_2 on geological time scales through feedbacks associated with C_{org} burial rates.

A drop in Po_2 over the past 800,000 years due solely to changes in C_{org} burial versus oxidation rates (regardless of the cause) requires positive CO_2 fluxes ($\sim 3 \times 10^{11}$ moles C per year) into the ocean and atmosphere ([19](#)). However, ice core records of past carbon dioxide partial pressures (PCO_2) show no obvious change in the mean over the past 800,000 years ([37–39](#)) ([Fig. 3](#)). To understand how changes in Po_2 influence PCO_2 , we developed a simple model of the carbon cycle that allows for changes in weathering and burial rates of carbonates, C_{org} , and silicates ([19](#)). In the absence of any PCO_2 -dependent feedbacks, a constant decline in $\delta O_2/N_2$ of 8.4‰ over the past million years from a net imbalance in C_{org} fluxes causes PCO_2 to rise by ~140

parts per million over the same time frame. Such a rise is inconsistent with the P_{CO_2} record (**Fig. 3**). A P_{CO_2} -dependent silicate weathering feedback (**40**) can account for the higher CO_2 flux if silicate weathering is enhanced by ~6% relative to volcanic outgassing. For example, response times for silicate weathering of 200,000 to 500,000 years (**41**) stabilize P_{CO_2} levels within ~1 million years (**Fig. 3**).

Changes in Cenozoic climate began millions of years before the start of our ice core-based $\delta O_2/N_2$ record 800,000 years ago (e.g., **2, 30, 34, 35**). Thus, we suggest that modest enhancements in silicate weathering would already have stabilized the portion of the P_{CO_2} ice core record that is controlled by differences in C_{org} and pyrite burial and oxidation. Thus, the combination of changing P_{O_2} and constant average P_{CO_2} provides distinctive evidence for feedbacks that regulate P_{CO_2} on geologic time scales (**37**). Lastly, a 2% imbalance in O_2 fluxes results in only a ~0.1‰ shift in the $^{13}C/^{12}C$ ratio of buried carbon (**19**).

- [Download high-res image](#)
- [Open in new tab](#)
- [Download Powerpoint](#)

Fig. 3 Comparison of calculated and measured P_{CO_2} values due to declining P_{O_2} with and without a P_{CO_2} -dependent silicate weathering feedback.

Inclusion of a silicate weathering feedback with geologically reasonable response times [200,000 to 500,000 years (**41**)] stabilizes P_{CO_2} within ~1 million years. Thus, increased silicate weathering rates could have compensated for enhanced CO_2 fluxes from increased net C_{org} oxidation more than 800,000 years ago. The P_{CO_2} records are continuous only from 800,000 years to the present. The model used to calculate P_{CO_2} values is described in (**19**); the measured P_{CO_2} values are from (**38**) and (**39**). ppm, parts per million.

Our results provide a primary record of declining P_{O_2} over the past 800,000 years sustained by a ~2% imbalance between O_2 sources and sinks. Critically, this decline is consistent with previously proposed and relatively simple models that invoke either the effects of increased Pleistocene erosion rates or decreased ocean temperature to explain feedbacks in the global cycles of carbon, sulfur, and O_2 —and the effects of both could have contributed to the observed decline in P_{O_2} . Regardless, creating primary records of past P_{O_2} is the necessary first step in identifying the fundamental processes that regulate P_{O_2} on geological time scales. Given evidence that both global erosion rates and temperature have changed markedly over the

Cenozoic ([42](#)), the ideas presented here may have implications for the history of Po_2 beyond the Pleistocene.

SUPPLEMENTARY MATERIALS

www.sciencemag.org/content/353/6306/1427/suppl/DC1

Materials and Methods

Figs. S1 to S6

Tables S1 to S3

References ([43–78](#))

REFERENCES AND NOTES

1. [!\[\]\(0f48f43ebd21f231a458c96216dbf4d1_img.jpg\)](#)
 1. L. R. Kump,
 2. R. M. Garrels , Modeling atmospheric O₂ in the global sedimentary redox cycle. Am. J. Sci. **286**, 337–360 (1986).doi:10.2475/ajs.286.5.337
[Abstract](#)/[FREE Full Text](#)[Google Scholar](#)
2. [!\[\]\(ba0878532603d6e0b20c60ffb7475d12_img.jpg\)](#)
 1. N. Shackleton , The carbon isotope record of the Cenozoic: History of organic carbon burial and of oxygen in the ocean and atmosphere. Geol. Soc. Lond. Spec. Publ. **26**, 423–434 (1987).doi:10.1144/GSL.SP.1987.026.01.27
[Abstract](#)/[FREE Full Text](#)[Google Scholar](#)
3.
 1. R. A. Berner,
 2. D. E. Canfield , A new model for atmospheric oxygen over Phanerozoic time. Am. J. Sci. **289**, 333–361 (1989).doi:10.2475/ajs.289.4.333pmid:11539776
[CrossRef](#)[PubMed](#)[Web of Science](#)[Google Scholar](#)
4.
 1. L. A. Derry,
 2. C. France-Lanord

, Neogene growth of the sedimentary organic carbon reservoir. *Paleoceanography* **11**, 267–275 (1996). doi:10.1029/95PA03839

[CrossRef](#)[Web of Science](#)[Google Scholar](#)

5.

1. K. W. Hansen,
2. K. Wallmann

, Cretaceous and Cenozoic evolution of seawater composition, atmospheric O₂ and CO₂: A model perspective. *Am. J. Sci.* **303**, 94–148 (2003). doi:10.2475/ajs.303.2.94

[Abstract](#)[/FREE Full Text](#)[Google Scholar](#)

6.

1. N. M. Bergman,
2. T. M. Lenton,
3. A. J. Watson

, COPSE: A new model of biogeochemical cycling over Phanerozoic time. *Am. J. Sci.* **304**, 397–437(2004). doi:10.2475/ajs.304.5.397

[Abstract](#)[/FREE Full Text](#)[Google Scholar](#)

7. ↵

1. P. G. Falkowski,
2. M. E. Katz,
3. A. J. Milligan,
4. K. Fennel,
5. B. S. Cramer,
6. M. P. Aubry,
7. R. A. Berner,
8. M. J. Novacek,
9. W. M. Zapol

, The rise of oxygen over the past 205 million years and the evolution of large placental mammals. *Science* **309**, 2202–2204 (2005). doi:10.1126/science.1116047 pmid:16195457

[Abstract](#)[/FREE Full Text](#)[Google Scholar](#)

8.

1. R. S. Arvidson,
2. F. T. Mackenzie,

3. M. Guidry

, MAGic: A Phanerozoic model for the geochemical cycling of major rock-forming components. Am. J. Sci. **306**, 135–190 (2006). doi:10.2475/ajs.306.3.135

[Abstract](#)/[FREE Full Text](#)[Google Scholar](#)

9.

1. R. A. Berner

, GEOCARBSULF: A combined model for Phanerozoic atmospheric O₂ and CO₂. Geochim. Cosmochim. Acta **70**, 5653–5664(2006).

[CrossRef](#)[Web of Science](#)[Google Scholar](#)

10. [!\[\]\(001c507f0f5ed6994b55b52cf164d44f_img.jpg\)](#)

1. R. A. Berner

, Phanerozoic atmospheric oxygen: New results using the GEOCARBSULF model. Am. J. Sci. **309**, 603–606 (2009).doi:10.2475/07.2009.03

[Abstract](#)/[FREE Full Text](#)[Google Scholar](#)

11.

1. I. J. Glasspool,

2. A. C. Scott

, Phanerozoic concentrations of atmospheric oxygen reconstructed from sedimentary charcoal. Nat. Geosci. **3**, 627–630(2010). doi:10.1038/ngeo923

[CrossRef](#)[Google Scholar](#)

12. [!\[\]\(79aedf6e8ebc80ad48544811a099141e_img.jpg\)](#)

1. R. Tappert,

2. R. C. McKellar,

3. A. P. Wolfe,

4. M. C. Tappert,

5. J. Ortega-Blanco,

6. K. Muehlenbachs

, Stable carbon isotopes of C₃ plant resins and ambers record changes in atmospheric oxygen since the Triassic. Geochim. Cosmochim. Acta **121**, 240–262 (2013). doi:10.1016/j.gca.2013.07.011

[CrossRef](#)[Google Scholar](#)

13. [!\[\]\(2a9609cc06bd3cbab56c9f0f9b6ea755_img.jpg\)](#)

1. M. L. Bender

, Orbital tuning chronology for the Vostok climate record supported by trapped gas composition. *Earth Planet. Sci. Lett.* **204**, 275–289(2002). doi:10.1016/S0012-821X(02)00980-9

[CrossRef](#)[Google Scholar](#)

14. ↵

1. K. Kawamura,
2. F. Parrenin,
3. L. Lisiecki,
4. R. Uemura,
5. F. Vimeux,
6. J. P. Severinghaus,
7. M. A. Hutterli,
8. T. Nakazawa,
9. S. Aoki,
10. J. Jouzel,
11. M. E. Raymo,
12. K. Matsumoto,
13. H. Nakata,
14. H. Motoyama,
15. S. Fujita,
16. K. Goto-Azuma,
17. Y. Fujii,
18. O. Watanabe

, Northern Hemisphere forcing of climatic cycles in Antarctica over the past 360,000 years. *Nature* **448**, 912–916 (2007). doi:10.1038/nature06015 pmid:17713531

[CrossRef](#)[PubMed](#)[Google Scholar](#)

15. ↵

1. M. Suwa,
2. M. L. Bender

, Chronology of the Vostok ice core constrained by O₂/N₂ ratios of occluded air, and its implication for the Vostok climate records. *Quat. Sci. Rev.* **27**, 1093–1106 (2008). doi:10.1016/j.quascirev.2008.02.017

[CrossRef](#)[Google Scholar](#)

16. [!\[\]\(e534b81ebbcbffc535c1288bc3986668_img.jpg\)](#)

1. A. Landais,
2. G. Dreyfus,
3. E. Capron,
4. K. Pol,
5. M. F. Loutre,
6. D. Raynaud,
7. V. Y. Lipenkov,
8. L. Arnaud,
9. V. Masson-Delmotte,
10. D. Paillard,
11. J. Jouzel,
12. M. Leuenberger

, Towards orbital dating of the EPICA Dome C ice core using $\delta\text{O}_2/\text{N}_2$. Clim. Past **8**, 191–203 (2012). doi:10.5194/cp-8-191-2012
[CrossRef](#) [Google Scholar](#)

17. [!\[\]\(d20711c6bdfea8f923f17f31b1eefa2d_img.jpg\)](#)

1. L. Bazin,
2. A. Landais,
3. E. Capron,
4. V. Masson-Delmotte,
5. C. Ritz,
6. G. Picard,
7. J. Jouzel,
8. M. Dumont,
9. M. Leuenberger,
10. F. Prié

, Phase relationships between orbital forcing and the composition of air trapped in Antarctic ice cores. Clim. Past **12**, 729–748 (2016). doi:10.5194/cp-12-729-2016
[CrossRef](#) [Google Scholar](#)

18. [!\[\]\(933d52e6c138874f3a19317302c3d001_img.jpg\)](#)

M. E. Smith, thesis, Princeton University, Princeton, NJ (1998).

[Google Scholar](#)

19. ↵ Materials and methods are available as supplementary materials on *Science Online*.

20. ↵

1. M. Battle,
2. M. Bender,
3. T. Sowers,
4. P. P. Tans,
5. J. H. Butler,
6. J. W. Elkins,
7. J. T. Ellis,
8. T. Conway,
9. N. Zhang,
10. P. Lang,
11. A. D. Clarket

, Atmospheric gas concentrations over the past century measured in air from firn at the South Pole. *Nature* **383**, 231 (1996). doi:10.1038/383231a0

[CrossRef](#) [Web of Science](#) [Google Scholar](#)

21. ↵

1. M. Bender,
2. T. Sowers,
3. V. Lipenkov

, On the concentrations of O₂, N₂, and Ar in trapped gases from ice cores. *J. Geophys. Res. Atmos.* **100**, 18651–18660 (1995). doi:10.1029/94JD02212

[CrossRef](#) [Google Scholar](#)

22. ↵

1. T. Kobashi,
2. T. Ikeda-Fukazawa,
3. M. Suwa,
4. J. Schwander,
5. T. Kameda,

6. J.Lundin,
7. A. Hori,
8. H. Motoyama,
9. M. Döring,
10. M. Leuenberger

, Post-bubble close-off fractionation of gases in polar firn and ice cores: Effects of accumulation rate on permeation through overloading pressure. *Atmos. Chem. Phys.* **15**, 13895–13914 (2015). doi:10.5194/acp-15-13895-2015
[CrossRef](#)[Google Scholar](#)

23. [!\[\]\(869f8db8cb6058a4d20fc99f4521bf06_img.jpg\)](#)

1. J. P. Severinghaus,
2. R. Beaudette,
3. M. A. Headly,
4. K. Taylor,
5. E. J. Brook

, Oxygen-18 of O₂ records the impact of abrupt climate change on the terrestrial biosphere. *Science* **324**, 1431–1434 (2009). doi:10.1126/science.1169473 pmid:19520957
[Abstract/FREE Full Text](#)[Google Scholar](#)

24. [!\[\]\(f024d36410e36011059c73f7d7908105_img.jpg\)](#)

1. H. Craig,
2. Y. Horibe,
3. T. Sowers

, Gravitational separation of gases and isotopes in polar ice caps. *Science* **242**, 1675–1678 (1988). doi:10.1126/science.242.4886.1675 pmid:17730578
[Abstract/FREE Full Text](#)[Google Scholar](#)

25. [!\[\]\(2becda4813f27b5edb43f5299d7596ac_img.jpg\)](#)

1. R. A. Berner

, Geological nitrogen cycle and atmospheric N₂ over Phanerozoic time. *Geology* **34**, 413–415 (2006). doi:10.1130/G22470.1
[Abstract/FREE Full Text](#)[Google Scholar](#)

26. [!\[\]\(f30959f11bdeaf28e16bccc4e6d35d33_img.jpg\)](#)

1. H. D. Holland

, Volcanic gases, black smokers, and the Great Oxidation Event. *Geochim. Cosmochim. Acta* **66**, 3811–3826 (2002).
[CrossRef](#)[Web of Science](#)[Google Scholar](#)

27. ↵The imbalance is calculated as follows: The total imbalance (moles per million years) for O₂ is $0.0084 \times n_{O_2}$, where n_{O_2} is the total number of moles of O₂ in the atmosphere. The O₂ flux is n_{O_2} divided by its residence time. The residence time of O₂ is about 2 million years. The percent imbalance is the total imbalance divided by the total flux, or $0.0084n_{O_2}/(n_{O_2}/2) = 0.017$ (1.7%).

28. ↵

1. F. Herman,
2. D. Seward,
3. P. G. Valla,
4. A. Carter,
5. B. Kohn,
6. S. D. Willett,
7. T. A. Ehlers

, Worldwide acceleration of mountain erosion under a cooling climate. *Nature* **504**, 423–426 (2013). doi:10.1038/nature12877pmid:24352288

[CrossRef](#)[PubMed](#)[Web of Science](#)[Google Scholar](#)

29. ↵

1. J. K. Willenbring,
2. F. von Blanckenburg

, Long-term stability of global erosion rates and weathering during late-Cenozoic cooling. *Nature* **465**, 211–

214 (2010). doi:10.1038/nature09044pmid:20463736

[CrossRef](#)[PubMed](#)[Web of Science](#)[Google Scholar](#)

30. ↵

1. M. A. Torres,
2. A. J. West,
3. G. Li

, Sulphide oxidation and carbonate dissolution as a source of CO₂ over geological timescales. *Nature* **507**, 346–

349 (2014). doi:10.1038/nature13030pmid:24646998

[CrossRef](#)[PubMed](#)[Google Scholar](#)

31. ↵
1. A. S. Colman,
 2. F. T. Mackenzie,
 3. H. D. Holland
- , Redox stabilization of the atmosphere and oceans and marine productivity. *Science* **275**, 406-407(1997). doi:10.1126/science.275.5298.406pmid:11536784
[Abstract](#)/[FREE Full Text](#)/[Google Scholar](#)
32. ↵
1. P. Van Cappellen,
 2. E. D. Ingall
- , Redox stabilization of the atmosphere and oceans by phosphorus-limited marine productivity. *Science* **271**, 493-496(1996). doi:10.1126/science.271.5248.493pmid:11541251
[Abstract](#)/[Google Scholar](#)
33. ↵
1. J. I. Hedges,
 2. R. G. Keil
- , Sedimentary organic matter preservation: An assessment and speculative synthesis. *Mar. Chem.* **49**, 81-115 (1995).doi:10.1016/0304-4203(95)00008-F
[CrossRef](#)/[Web of Science](#)/[Google Scholar](#)
34. ↵
1. C. H. Lear,
 2. H. Elderfield,
 3. P. A. Wilson
- , Cenozoic deep-sea temperatures and global ice volumes from Mg/Ca in benthic foraminiferal calcite. *Science* **287**, 269-272 (2000). doi:10.1126/science.287.5451.269pmid:10634774
[Abstract](#)/[FREE Full Text](#)/[Google Scholar](#)
35. ↵
1. B. Cramer,
 2. K. Miller,
 3. P. Barrett,

4. J. Wright

, Late Cretaceous–Neogene trends in deep ocean temperature and continental ice volume: Reconciling records of benthic foraminiferal geochemistry ($\delta^{18}\text{O}$ and Mg/Ca) with sea level history. *J. Geophys. Res. Oceans* **116**, C12023 (2011).

[CrossRef](#)[Google Scholar](#)

36. [!\[\]\(30721963adf153ec6da28290a8354fb9_img.jpg\)](#)

1. H. E. Garcia,
2. L. I. Gordon

, Oxygen solubility in seawater: Better fitting equations. *Limnol. Oceanogr.* **37**, 1307–1312 (1992). doi:10.4319/lo.1992.37.6.1307

[CrossRef](#)[Web of Science](#)[Google Scholar](#)

37. [!\[\]\(23570f0bb23cd13b166a0be3a30a90a9_img.jpg\)](#)

1. R. E. Zeebe,
2. K. Caldeira

, Close mass balance of long-term carbon fluxes from ice-core CO₂ and ocean chemistry records. *Nat. Geosci.* **1**, 312–315(2008). doi:10.1038/ngeo185

[CrossRef](#)[Google Scholar](#)

38. [!\[\]\(f5e8494903a4a2e18e65df81080563be_img.jpg\)](#)

1. B. Bereiter,
2. S. Eggleston,
3. J. Schmitt,
4. C. Nehrbass-Ahles,
5. T. F. Stocker,
6. H. Fischer,
7. S. Kipfstuhl,
8. J. Chappellaz

, Revision of the EPICA Dome C CO₂ record from 800 to 600 kyr before present. *Geophys. Res. Lett.* **42**, 542–549(2015). doi:10.1002/2014GL061957

[CrossRef](#)[Google Scholar](#)

39. [!\[\]\(c3723390e7fae1fcf0aa666259958e76_img.jpg\)](#)

1. J. A. Higgins,
2. A. V. Kurbatov,

3. N. E. Spaulding,
4. E. Brook,
5. D. S. Introne,
6. L. M. Chimiak,
7. Y. Yan,
8. P. A. Mayewski,
9. M. L. Bender

, Atmospheric composition 1 million years ago from blue ice in the Allan Hills, Antarctica. Proc. Natl. Acad. Sci. U.S.A. **112**, 6887–6891 (2015). doi:10.1073/pnas.1420232112pmid:25964367

[Abstract](#)/[FREE Full Text](#)[Google Scholar](#)

40. 

1. J. C. Walker,
2. P. Hays,
3. J. Kasting

, A negative feedback mechanism for the long-term stabilization of the Earth's surface temperature. J. Geophys. Res. **86**, 9776–9782 (1981). doi:10.1029/JC086iC10p09776

[CrossRef](#)[Web of Science](#)[Google Scholar](#)

41. 

1. D. Archer

, Fate of fossil fuel CO₂ in geologic time. J. Geophys. Res. Oceans **110**, C09S05 (2005).

[Google Scholar](#)

42. 

1. M. Raymo,
2. W. F. Ruddiman

, Tectonic forcing of late Cenozoic climate. Nature **359**, 117–122 (1992). doi:10.1038/359117a0

[CrossRef](#)[Web of Science](#)[Google Scholar](#)

43. 

1. M. L. Bender,
2. B. Barnett,
3. G. Dreyfus,

4. J. Jouzel,
 5. D. Porcelli
- , The contemporary degassing rate of ^{40}Ar from the solid Earth. Proc. Natl. Acad. Sci. U.S.A. **105**, 8232–8237 (2008). doi:10.1073/pnas.0711679105 pmid:18550816
[Abstract](#)/[FREE Full Text](#)[Google Scholar](#)

- 44.
1. R. F. Keeling,
 2. S. C. Piper,
 3. M. Heimann
- , Global and hemispheric CO_2 sinks deduced from changes in atmospheric O_2 concentration. Nature **381**, 218–221 (1996). doi:10.1038/381218a0
[CrossRef](#)[Web of Science](#)[Google Scholar](#)

- 45.
1. M. L. Bender,
 2. D. T. Ho,
 3. M. B. Hendricks,
 4. R. Mika,
 5. M. O. Battle,
 6. P. P. Tans,
 7. T. J. Conway,
 8. B. Sturtevant,
 9. N. Cassar
- , . Atmospheric O_2/N_2 changes, 1993–2002: Implications for the partitioning of fossil fuel CO_2 sequestration. Global Biogeochem. Cycles **19**, GB4017 (2005).
[Google Scholar](#)

- 46.
1. R. Keeling,
 2. A. Manning
- , Studies of recent changes in atmospheric O_2 content. Treatise Geochem. **4**, 385–404 (2014). doi:10.1016/B978-0-08-095975-7.00420-4
[CrossRef](#)[Google Scholar](#)

- 47.
1. R. F. Keeling,
 2. S. R. Shertz
- , Seasonal and interannual variations in atmospheric oxygen and implications for the global carbon cycle. *Nature* **358**, 723–727 (1992). doi:10.1038/358723a0
[CrossRef](#)[Google Scholar](#)
- 48.
1. T. Sowers,
 2. M. Bender,
 3. D. Raynaud
- , Elemental and isotopic composition of occluded O₂ and N₂ in polar ice. *J. Geophys. Res. Atmos.* **94**, 5137–5150(1989). doi:10.1029/JD094iD04p05137
[CrossRef](#)[Web of Science](#)[Google Scholar](#)
- 49.
1. T. Ikeda,
 2. H. Fukazawa,
 3. S. Mae,
 4. L. Pepin,
 5. P. Duval,
 6. B. Champagnon,
 7. V. Y. Lipenkov,
 8. T. Hondoh
- , Extreme fractionation of gases caused by formation of clathrate hydrates in Vostok Antarctic ice. *Geophys. Res. Lett.* **26**, 91–94(1999). doi:10.1029/1998GL900220
[CrossRef](#)[Google Scholar](#)
50. G. Dreyfus, thesis, Princeton University, Princeton, NJ (2008).
[Google Scholar](#)
51. M. Suwa, thesis, Princeton University, Princeton, NJ (2007).
[Google Scholar](#)
- 52.

1. J.-R. Petit,
2. J. Jouzel,
3. D. Raynaud,
4. N. I. Barkov,
5. J.-M. Barnola,
6. I. Basile,
7. M. Bender,
8. J. Chappellaz,
9. M. Davis,
10. G. Delaygue,
11. M. Delmotte,
12. V. M. Kotlyakov,
13. M. Legrand,
14. V. Y. Lipenkov,
15. C. Lorius,
16. L. PÉpin,
17. C. Ritz,
18. E. Saltzman,
19. M. Stievenard

, Climate and atmospheric history of the past 420,000 years from the Vostok ice core, Antarctica. *Nature* **399**, 429–436 (1999). doi:10.1038/20859
[CrossRef](#) [Web of Science](#) [Google Scholar](#)

53.

1. F. Parrenin,
2. J. Jouzel,
3. C. Waelbroeck,
4. C. Ritz,
5. J. M. Barnola

, Dating the Vostok ice core by an inverse method. *J. Geophys. Res. Atmos.* **106**, 31837–31851(2001). doi:10.1029/2001JD900245
[CrossRef](#) [Google Scholar](#)

54.

1. L. Bazin,

2. A. Landais,
3. B. Lemieux-Dudon,
4. H. Toyé Mahamadou Kele,
5. D. Veres,
6. F. Parrenin,
7. P. Martinerie,
8. C. Ritz,
9. E. Capron,
10. V. Lipenkov,
11. M.-F. Loutre,
12. D. Raynaud,
13. B. Vinther,
14. A. Svensson,
15. S. O. Rasmussen,
16. M. Severi,
17. T. Blunier,
18. M. Leuenberger,
19. H. Fischer,
20. V. Masson-Delmotte,
21. J. Chappellaz,
22. E. Wolff

, An optimized multi-proxy, multi-site Antarctic ice and gas orbital chronology (AICC2012): 120–800 ka. *Clim. Past* **9**, 1715–1731 (2013). doi:10.5194/cp-9-1715-2013

[CrossRef](#) [Web of Science](#) [Google Scholar](#)

- 55.

 1. D. Veres,
 2. L. Bazin,
 3. A. Landais,
 4. H. Toyé Mahamadou Kele,
 5. B. Lemieux-Dudon,
 6. F. Parrenin,
 7. P. Martinerie,

8. E. Blayo,
9. T. Blunier,
10. E. Capron,
11. J. Chappellaz,
12. S. O.Rasmussen,
13. M. Severi,
14. A. Svensson,
15. B. Vinther,
16. E. W. Wolff

, The Antarctic ice core chronology (AICC2012): An optimized multi-parameter and multi-site dating approach for the last 120 thousand years. *Clim. Past* **9**, 1733–1748(2013). doi:10.5194/cp-9-1733-2013
[CrossRef](#)[Web of Science](#)[Google Scholar](#)

56.

1. M. Bender,
2. T. Sowers,
3. M.-L. Dickson,
4. J. Orchardo,
5. P. Grootes,
6. P. A. Mayewski,
7. D. A. Meese

, Climate correlations between Greenland and Antarctica during the past 100,000 years. *Nature* **372**, 663–666 (1994).doi:10.1038/372663a0
[CrossRef](#)[Google Scholar](#)

57. D. Meese, “Preliminary depth-age scale of the GISP2 ice core” (U.S. Army Corps of Engineers, Cold Regions Research and Engineering Laboratory, 1994).

[Google Scholar](#)

58.

1. D. Meese,
2. A. J. Gow,
3. R. B. Alley,
4. G. A. Zielinski,

5. P. M. Grootes,
6. M. Ram,
7. K. C. Taylor,
8. P. A. Mayewski,
9. J. F. Bolzan

, The Greenland Ice Sheet Project 2 depth-age scale: Methods and results. *J. Geophys. Res. Oceans* **102**, 26411–26423(1997). doi:10.1029/97JC00269

[CrossRef](#)[Google Scholar](#)

59.

1. T. Sowers,
2. M. Bender,
3. D. Raynaud,
4. Y. Korotkevich

, $\delta^{15}\text{N}$ of N_2 in air trapped in polar ice: A tracer of gas transport in the firn and a possible constraint on ice age-gas age differences. *J. Geophys. Res. Atmos.* **97**, 15683–15697 (1992). doi:10.1029/92JD01297

[CrossRef](#)[Web of Science](#)[Google Scholar](#)

60.

1. S. Fujita,
2. J. Okuyama,
3. A. Hori,
4. T. Hondoh

, Metamorphism of stratified firn at Dome Fuji, Antarctica: A mechanism for local insolation modulation of gas transport conditions during bubble close off. *J. Geophys. Res. Earth Surf.* **114**, F03023 (2009).

[CrossRef](#)[Google Scholar](#)

61.

1. D. Paillard,
2. L. Labeyrie,
3. P. Yiou

, Macintosh program performs time-series analysis. *Eos Trans. AGU* **77**, 379 (1996). doi:10.1029/96EO00259

[CrossRef](#)[Google Scholar](#)

- 62.
1. J. Laskar,
 2. P. Robutel,
 3. F. Joutel,
 4. M. Gastineau,
 5. A. C. M. Correia,
 6. B. Levrard
- , A long-term numerical solution for the insolation quantities of the Earth. *Astron. Astrophys.* **428**, 261–285 (2004). doi:10.1051/0004-6361:20041335
[CrossRef](#) [Web of Science](#) [Google Scholar](#)
63. D. Gough, in *Physics of Solar Variations* (Springer, 1981), pp. 21–34.
[Google Scholar](#)
- 64.
1. T. Sowers,
 2. E. Brook,
 3. D. Etheridge,
 4. T. Blunier,
 5. A. Fuchs,
 6. M. Leuenberger,
 7. J. Chappellaz,
 8. J. M. Barnola,
 9. M. Wahlen,
 10. B. Deck,
 11. C. Weyhenmeyer
- , An interlaboratory comparison of techniques for extracting and analyzing trapped gases in ice cores. *J. Geophys. Res. Oceans* **102**, 26527–26538(1997). doi:10.1029/97JC00633
[CrossRef](#) [Google Scholar](#)
- 65.
1. C. Huber,
 2. U. Beyerle,
 3. M. Leuenberger,

4. J. Schwander,
5. R. Kipfer,
6. R. Spahni,
7. J. Severinghaus,
8. K. Weiler

, Evidence for molecular size dependent gas fractionation in firn air derived from noble gases, oxygen, and nitrogen measurements. *Earth Planet. Sci. Lett.* **243**, 61–73 (2006).doi:10.1016/j.epsl.2005.12.036
[CrossRef](#)[Google Scholar](#)

66.

1. J. P. Severinghaus,
2. M. O. Battle

, Fractionation of gases in polar ice during bubble close-off: New constraints from firn air Ne, Kr and Xe observations. *Earth Planet. Sci. Lett.* **244**, 474–500 (2006).doi:10.1016/j.epsl.2006.01.032
[CrossRef](#)[Google Scholar](#)

67.

1. J. P. Severinghaus,
2. T. Sowers,
3. E. J. Brook,
4. R. B. Alley,
5. M. L. Bender

, Timing of abrupt climate change at the end of the Younger Dryas interval from thermally fractionated gases in polar ice. *Nature* **391**, 141–146 (1998).doi:10.1038/34346
[CrossRef](#)[Web of Science](#)[Google Scholar](#)

68.

1. J. P. Severinghaus,
2. M. L. Bender,
3. R. F. Keeling,
4. W. S. Broecker

, Fractionation of soil gases by diffusion of water vapor, gravitational settling, and thermal diffusion. *Geochim. Cosmochim. Acta* **60**, 1005–1018 (1996).

[CrossRef](#)[Web of Science](#)[Google Scholar](#)

- 69.
1. M. Battle,
 2. M. Bender,
 3. M. B. Hendricks,
 4. D. T. Ho,
 5. R. Mika,
 6. G. McKinley,
 7. S.-M. Fan,
 8. T. Blaine,
 9. R. F. Keeling
- , Measurements and models of the atmospheric Ar/N₂ ratio. *Geophys. Res. Lett.* **30**, 1786 (2003).
[Google Scholar](#)
- 70.
1. J. P. Severinghaus,
 2. A. Grachev,
 3. M. Battle
- , Thermal fractionation of air in polar firn by seasonal temperature gradients. *Geochem. Geophys. Geosyst.* **2**, 2000GC000146 (2001). doi:10.1029/2000GC000146
[CrossRef](#)[Google Scholar](#)
- 71.
1. T. A. Laakso,
 2. D. P. Schrag
- , Regulation of atmospheric oxygen during the Proterozoic. *Earth Planet. Sci. Lett.* **388**, 81–91 (2014). doi:10.1016/j.epsl.2013.11.049
[CrossRef](#)[Google Scholar](#)
- 72.
1. A. Bachan,
 2. L. R. Kump
- , The rise of oxygen and siderite oxidation during the Lomagundi Event. *Proc. Natl. Acad. Sci. U.S.A.* **112**, 6562–6567 (2015). doi:10.1073/pnas.1422319112 pmid:25964326
[Abstract/FREE Full Text](#)[Google Scholar](#)

73.

1. R. N. Roy,
2. L. N. Roy,
3. K. M. Vogel,
4. C. Porter-Moore,
5. T. Pearson,
6. C. E. Good,
7. F. J. Millero,
8. D. M. Campbell

, The dissociation constants of carbonic acid in seawater at salinities 5 to 45 and temperatures 0 to 45 C. Mar. Chem. **44**, 249–267 (1993). doi:10.1016/0304-4203(93)90207-5

[CrossRef](#)[Web of Science](#)[Google Scholar](#)

74. R. E. Zeebe, D. A. Wolf-Gladrow, *CO₂ in Seawater: Equilibrium, Kinetics, Isotopes* (Oceanography Series 65, Elsevier, 2001).

[Google Scholar](#)

75.

1. J. M. Hayes,
2. H. Strauss,
3. A. J. Kaufman

, The abundance of ¹³C in marine organic matter and isotopic fractionation in the global biogeochemical cycle of carbon during the past 800 Ma. Chem. Geol. **161**, 103–125 (1999). doi:10.1016/S0009-2541(99)00083-2

[CrossRef](#)[Web of Science](#)[Google Scholar](#)

76.

1. D. E. Canfield

, The early history of atmospheric oxygen: Homage to Robert M. Garrels. Annu. Rev. Earth Planet. Sci. **33**, 1–36 (2005). doi:10.1146/annurev.earth.33.092203.122711

[CrossRef](#)[Web of Science](#)[Google Scholar](#)

77.

1. M. Raymo,
2. D. Oppo,

3. W. Curry
, The mid-Pleistocene climate transition: A deep sea carbon isotopic perspective. *Paleoceanography* **12**, 546–559 (1997). doi:10.1029/97PA01019
[CrossRef](#)[Web of Science](#)[Google Scholar](#)

78. 

1. M. Suwa
, Termination V in the Vostok (Antarctica) ice core. *J. Glaciol.* **54**, 229–232 (2008). doi:10.3189/002214308784886153
[CrossRef](#)[Google Scholar](#)

Acknowledgments: D.A.S. acknowledges funding from a National Oceanic and Atmospheric Administration Climate & Global Change postdoctoral fellowship. J.A.H. and M.L.B. acknowledge support from National Science Foundation grant ANT-1443263. All data presented are available in the supplementary materials. We thank W. Fischer, I. Halevy, N. Planavsky, J. Severinghaus, and D. Sigman for helpful discussions and three anonymous reviewers for helpful comments on the manuscript. D.A.S., J.A.H., and M.L.B. conceived the study and wrote the manuscript. D.A.S., J.A.H., M.L.B., and Y.Y. analyzed the data. G.B.D. measured the Dome C $\delta\text{Ar}/\text{N}_2$ data. The views expressed in this article are those of the authors and do not necessarily represent the views of the Department of Energy or the U.S. Government.

[View Abstract](#)